Bulge-forming Galaxies with an Extended Rotating Disk at z ~ 2

Tadaki et al. 2017

2017ApJ...834..135T

arXiv:1608.05412

Presenter: K. Kushibiki

Contents

Abstract

ALMA observations at 870 um for 25 Hα-selected SFGs around MS at z=2.5-2.5

- **Dust emission** radiated from a single region close to the galaxy center
  - **Extremely compact** $R_{1/2,\,870\mu m} < 1.5\ \mathrm{kpc}$ (for 9 galaxies)
  - 2x smaller than rest-optical $\langle R_{1/2,\,1.6\mu m} \rangle = 3.2\ \mathrm{kpc}$
  - Comparable with optical size of massive quiescent at similar redshift
- They have **exponential disk** in rest-optical
  → Transition phase from extended disks to compact spheroids
- **High SFR density within the central 1 kpc**
  → Intense starbursts can rapidly build up a central bulge in several hundred Myr
- Ionized gas kinematics = **rotation-supported** with angular momentum ~ typical SFG

→ Bulges are commonly formed **in extended rotating disks by internal processes**

1. Introduction

SFGs
- Exponential disk
- Rotation
- Turbulent (high-z)

QGs
- Compact
- Cuspy

→ Quenching of SF must be accompanied by significant structural change

Two main evolutionary paths

1. Slow cosmological path: Galaxy size $R \propto (1+z)^{-1}$
   → Quench SF and add to the passive population in a later epoch
2. Fast path: Downward transition in the size-mass plane
   → Require "compaction"
   1. Major merger
   2. Internal angular momentum redistribution:
      Effective at high-redshift (gas-rich & effective viscous dissipation)
      May lead to inside-out quenching (Morphological quenching / AGN)

ALMA observation to search for compact concentrations of ISM as sign of fast paths

- Advantage: No selection bias in galaxy morphologies
- Key goal: Morphological transformation from extended exponential disk to spheroid

2. High-Resolution 870μm Imaging

2.1. Sample selection

- Narrow-band imaging survey with the MOIRCS in the SXDF-UDS-CANDELS field
  → 25 galaxies for ALMA observation
  - Prioritize bright object in MIPS 24μm maps (4 out of 25 are not detected at 24μm)

2.2. Galaxies properties

From 3D-HST catalog

- Stellar mass: SED fitting (BC03, Solar Metallicity, Exponentially declining SFH, Calzetti law)
- SFR: Combination of rest-2800AA and IR luminosity (PACS 160μm or MIPS 24μm)
  4 galaxies without IR detection: Hα-based SFR (dust correction with SED A_V)
- Structural parameters (half-light radius / Sersic index): GALFIT in HST/WFC3 H_{160}-band image

best sample: detected both in low-res and high-res 870 μm maps
detection: detected either map

Fig 1.

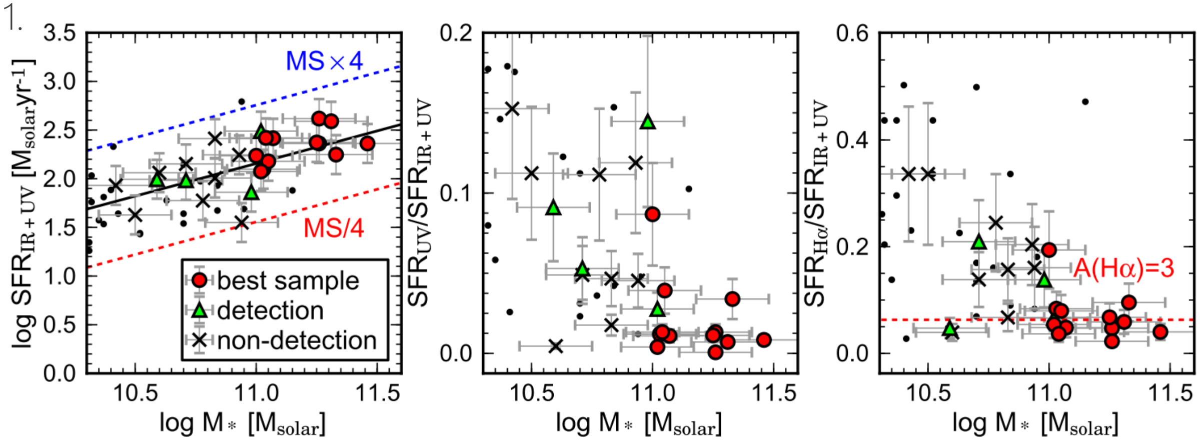

2. High-Resolution 870μm Imaging

2.3. ALMA observations

6-8 minutes, band 7, central frequency 345or350 GHz (~870μm)

→ Two kinds of clean maps

	Low-resolution map (uv-taper: on-sky FWHM=0".5)	High-resolution map (natural weighting)
Beam-size	0".47-0".54	0".15-0".21
Aperture for phot	1".5	1".0
RMS level of flux	98-142 μJy/beam	56-74 μJy/beam
Detection threshold	4σ	5σ

→ Detected 16 out of 25 galaxies

2.4. KMOS observations

Rotation velocity (v_{rot}) & Local velocity dispersion (σ_0)

- Determining radius at which velocity gradient reaches maximum: R_{max}
  → Rotation velocity at R_{max} and local velocity dispersion in outer disk

Specific angular momentum

- $j_{disk} = k_{disk} \times v_{circ} \times R_{1/2}$ (k_{disk}:correction of deviation from exponential profiles, v_{circ}: circular velocity corrected observational effect & turbulent pressure)

2. High-Resolution 870μm Imaging

Table 1.

3D-HST ID (Skelton+14)	$z_{\rm NB}$[a]	log M_*[b] ($M_\odot$)	log SFR[b] ($M_\odot {\rm yr}^{-1}$)	$\rm SNR_{0.5}$[c]	$\rm SNR_{0.2}$[c]	$S_{\rm aper}$[c] (mJy)	$S_{\rm model}$[d] (mJy)	$R_{1/2}$[d] (arcsec)	$R_{1/2,\rm cor}$[e] (arcsec)	$v_{\rm rot}/\sigma_0$[f]
U4-13952	2.19	11.33	2.25	13.4	7.9	2.51±0.31	2.94±0.55	0.24±0.04	0.28±0.06	3.8±1.3
U4-34817	2.19	11.26	2.36	7.8	5.4	1.73±0.28	2.13±0.78	0.31±0.10	0.38±0.12	Hα detection
U4-20704	2.19	11.46	2.36	8.1	6.3	3.00±0.40	4.28±1.11	0.44±0.10	0.48±0.11	4.2±1.4
U4-28702	2.19	11.03	2.10	10.1	9.7	1.73±0.36	1.64±0.31	0.10±0.02	0.13±0.03	
U4-36568	2.19	11.02	2.49	4.0	<5.0	0.71±0.24				5.3±1.8
U4-24247	2.19	10.71	1.98	4.4	<5.0	1.09±0.36				Hα detection
U4-32171	2.19	10.71	2.15	<4.0	<5.0					
U4-11582	2.19	10.83	2.01	<4.0	<5.0					6.9±2.4
U4-27289	2.19	10.78	1.78	<4.0	<5.0					
U4-36247	2.19	11.07	2.42	13.5	16.0	1.80±0.24	1.41±0.18	0.05±0.01	0.07±0.02	3.5±2.3
U4-32351	2.19	11.05	2.18	6.5	6.8	0.95±0.26	0.74±0.24	0.10±0.04	0.17±0.08	5.2±0.9
U4-18807	2.19	10.98	1.86	<4.0	5.5	0.58±0.26				7.1±4.9
U4-27939	2.19	10.60	2.06	<4.0	<5.0					
U4-14574	2.19	10.59	1.99	4.0	<5.0	1.20±0.46				
U4-15198	2.53	10.93	2.24	<4.0	<5.0					
U4-16795	2.53	11.26	2.62	31.0	29.2	4.59±0.31	4.46±0.27	0.12±0.01	0.13±0.01	
U4-34138	2.53	11.00	2.24	9.7	11.4	1.60±0.29	1.10±0.19	0.06±0.02	0.08±0.03	3.8±2.0
U4-28473	2.53	11.31	2.59	26.0	22.5	4.87±0.45	5.12±0.39	0.13±0.01	0.14±0.02	6.1±4.0
U4-33135	2.53	11.02	2.07	8.6	9.8	1.47±0.34	1.27±0.25	0.07±0.02	0.09±0.03	
U4-27046	2.53	10.83	2.41	<4.0	<5.0					Hα detection
U4-16504	2.53	11.25	2.37	20.4	15.7	2.82±0.23	3.16±0.34	0.15±0.02	0.17±0.03	
U4-11780	2.53	10.42	1.93	<4.0	<5.0					
U4-13197	2.53	10.94	1.55	<4.0	<5.0					
U4-34617	2.53	11.04	2.42	10.6	13.0	1.67±0.28	0.93±0.13	0.02±0.01	0.04±0.02	
U4-14870	2.53	10.50	1.63	<4.0	<5.0					

3. Spatial Extent of Star Formation within Galaxies

Where & how much stars are formed within galaxies at that epoch

→ With 870 µm maps tracing dust emission,
the spatial distributions of star formation within galaxies are studied.

For the best sample (detected in both in low-res & high-res map): 12 galaxies

3.1. High-resolution 870 µm maps

Visual inspection

- Little UV emission
  ← strong dust extinction
- 870 µm emission is radiated from a single region close to the rest-optical center
  → Primarily responsible for star formation in the galaxies

Fig 3.

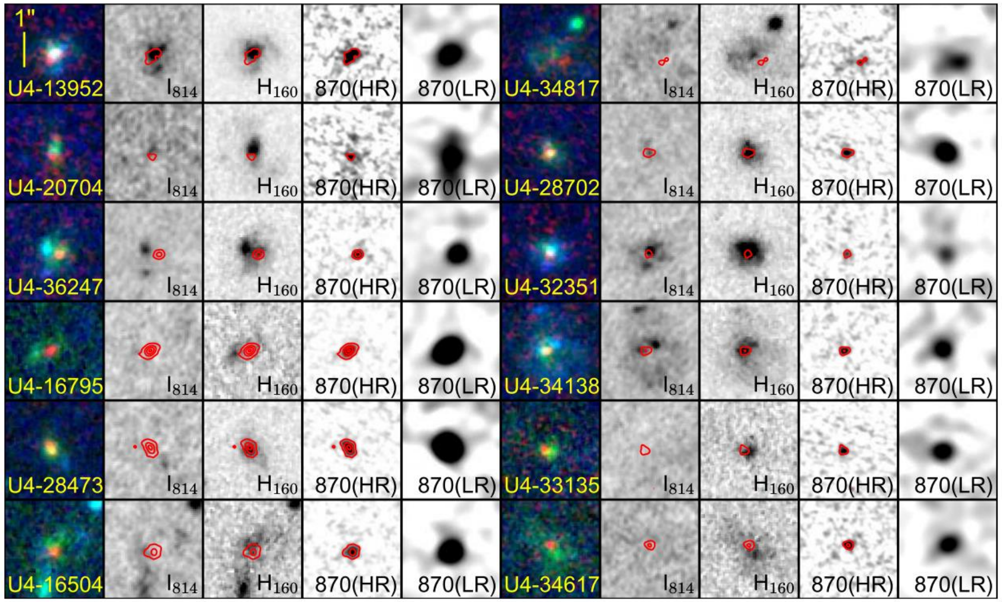

3. Spatial Extent of Star Formation within Galaxies

3.2. Size measurements for 870 μm continuum emission

Measured in the high-resolution map by visibility fitting with circular exponential profile

Exponential function in the image plane: $f(R) = \exp(-1.678R/R_{1/2})$

→ In the uv-plane: $g(u) = S_{\text{model}} \times \frac{k_0^3}{(u^2+k_0^2)^{3/2}}$

S_{model}: total flux of the model, k_0: spatial frequency to characterize a spatial extent

Impact of residual emission
(extended component, clumps,
or deviation from an exponential profile)

→ Stacking analysis of the model-subtracted visibilities for 9 compact sources

- 4.3σ detection of residual emission
- Within 2″ aperture $S_{\text{extra}} = 0.42$ mJy (21%)

Corrected half-light radius: $R_{1/2,\text{cor}}$

= radius enclosing $S_{1/2} = S_{\text{model}} + S_{\text{extra}}$
in the exponential component

Fig 4.

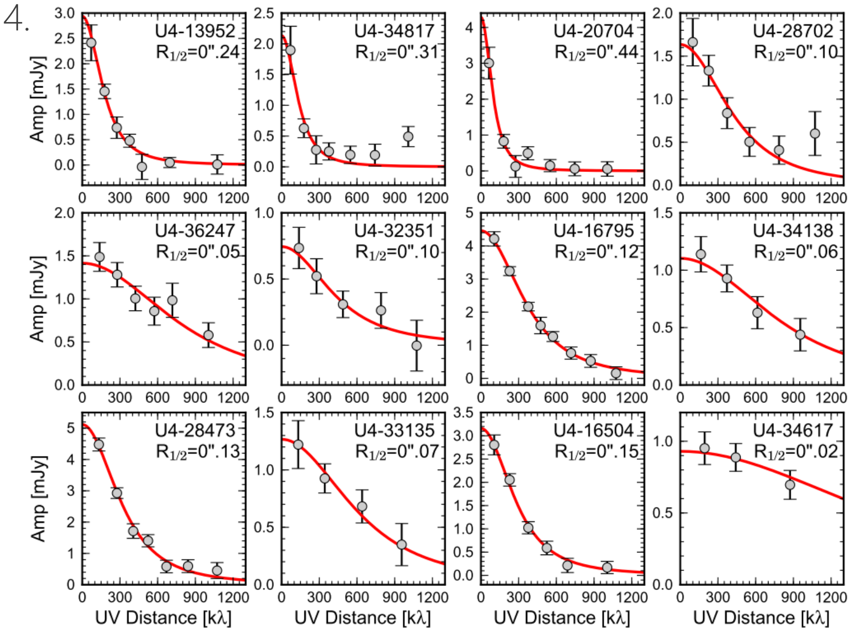

3. Spatial Extent of Star Formation within Galaxies

- For 9 of 12 galaxies, $R_{1/2,870\mu m} < 1.5$ kpc
  → 2x smaller than $R_{1/2,1.6\mu m}$ and comparable with optical sizes of massive quiescent galaxies
- All 12 galaxies are $\log(M_*/M_\odot) > 11$
  → Star formation preferentially occurs in the compact central region
  → Have potential to change morphology from disk-dominated to bulge-dominated
- 86% (12/14) massive galaxies are detected and have compact dust emission
  → Massive galaxies commonly form stars in the extremely compact central region
  (9/14 have $R_{1/2,870\mu m} < 1.5$ kpc)

→ These results agree with previous results (Barro+2016; pre-selecting optically compact SFGs)

Table 2.

3D-HST ID	$n_{1.6\mu m}$[a]	$R_{1/2,1.6\mu m}$[a] (kpc)	$R_{1/2,870\mu m}$[b] (kpc)	$\log\Sigma M_{*1\mathrm{kpc}}$[c] $M_\odot\,\mathrm{kpc}^{-2}$	$\log\Sigma\mathrm{SFR}_{1\mathrm{kpc}}$[d] $M_\odot\,\mathrm{yr}^{-1}\,\mathrm{kpc}^{-2}$	$\log\tau_{\mathrm{bulge}}$[e] (yr)	$\log\tau_{\mathrm{depl}}$[f] (yr)
U4-13952	2.2±0.2	3.6±0.2	2.3±0.5	9.63±0.15	1.00±0.23	8.96±0.26	8.56±0.31
U4-34817	0.6±0.6	5.0±0.5	3.1±1.0	9.17±0.15	0.93±0.30	9.14±0.30	8.48±0.31
U4-20704	3.4±0.2	5.8±0.8	4.0±0.9	9.83±0.15	0.72±0.26	8.96±0.41	8.55±0.31
U4-28702	1.2±0.5	2.5±0.3	1.0±0.3	9.45±0.15	1.28±0.22	8.79±0.23	8.52±0.31
U4-36247	0.5±0.4	2.9±0.3	0.6±0.2	9.68±0.15	1.76±0.20	8.19±0.25	8.39±0.31
U4-32351	1.9±0.8	2.6±0.2	1.4±0.6	9.56±0.15	1.28±0.24	8.74±0.26	8.49±0.31
U4-16795			1.0±0.1	9.38±0.15	1.81±0.20	8.29±0.21	8.34±0.31
U4-34138	1.2±0.2	5.8±0.4	0.6±0.2	9.41±0.15	1.55±0.21	8.55±0.21	8.41±0.31
U4-28473	1.5±1.2	2.4±0.5	1.2±0.1	9.73±0.15	1.73±0.20	8.16±0.27	8.37±0.31
U4-33135	1.0±2.1	1.5±0.8	0.8±0.2	9.76±0.15	1.36±0.21	8.50±0.29	8.49±0.31
U4-16504	1.0±0.8	3.1±0.8	1.4±0.2	9.46±0.15	1.43±0.21	8.64±0.22	8.44±0.31
U4-34617	0.9±0.3	5.0±0.7	0.3±0.2	9.17±0.15	1.76±0.20	8.40±0.20	8.35±0.31

Fig 5.

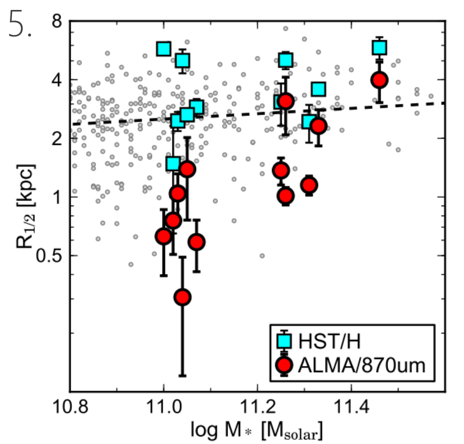

4. Bulge Formation in Extended, Rotating Disks

Massive ($\log(M_*/M_\odot)>11$) galaxies in this study are likely to soon quench

→ Centrally-concentrated star formation reduces the half-light radii or half-mass radii & their Sersic index would increase by central bulge formation

Possibility of bulge formation

Dense core of quiescent galaxies : $\log(\Sigma M_{*,1kpc}/M_\odot \mathrm{kpc}^{-2})=10$

Bulge formation timescale

$$\tau_{\mathrm{bulge}} = \frac{10^{10} - \Sigma M_{*,1\mathrm{kpc}}}{w \times \boxed{\Sigma \mathrm{SFR}_{1\mathrm{kpc}}}}$$

Resolved SED fitting with multi-band HST data

Distribute Spitzer/Herschel-based total SFR to the part of galaxies with best-fit exponential models at 870 μm

Mass loss due to stellar winds: $w = 0.6$

→ $\langle \log \tau_{\mathrm{bulge}} \rangle = 8.47\ (8.16 - 8.79)$ for the 9 galaxies

→ Complete dense core formation by z=2

Gas depletion timescale

Updated version of Genzel+2015 scaling relation (Tacconi+2018)

$$\log(M_{\mathrm{gas}}/\mathrm{SFR}) = 0.15\ - 0.79 \log(1+z) - 0.43 \log(\mathrm{sSFR}/\mathrm{sSFR}_{\mathrm{MS}}) + 0.06 \log(M_* - 10.5)$$

→ $\tau_{depl} = \frac{M_{\mathrm{gas}}}{\mathrm{SFR}(1+\eta)},\ \eta \sim 1$ (gas ejected by outflows)

$\langle \tau_{bulge}/\tau_{depl} \rangle \sim 1.2$ for 9 galaxies → The formation of a dense core doesn't require additional gas

4. Bulge Formation in Extended, Rotating Disks

Kinematic properties

6 galaxies are both in KMOS^{3D} and in 870 μm size measurement

- They are all rotation-supported ($v_{rot}/\sigma_0 > 3$)
- Span a range of disk angular momenta
  from local spirals to ellipticals
- Broadly consistent with the sample of KMOS3D

→ Not all galaxies with low angular momentum

→ Compact nuclear dust components are caused by internal angular momentum redistribution

Fig 6.

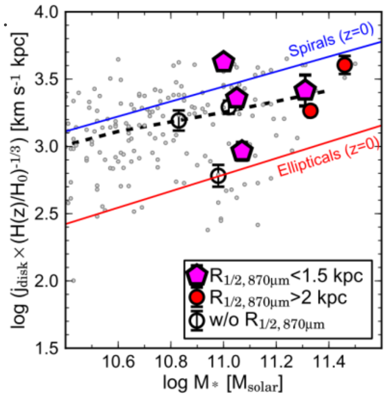

Halo mass

log($M_{halo}/M_\odot$) > 12 (Burkert+2016; KMOS observations and a Monte-Carlo modeling)

→ Virial shock suspend cold gas inflow

→ Naturally quench after the dense core formation

Galaxies with compact dust emission would be a key population
for morphological and star formation evolution from disks to quiescent spheroids

Galaxies with extended dust emission (remaining 3 galaxies)

- Two of them show $n_{Sersic} > 2$ → bulge is already formed

→ Become large quiescent galaxies (mode dominant at a later epoch)